Bimodality: A general feature of heavy ion reactions

A. Le Fèvre,[1,2] J. Aichelin,[1] C. Hartnack,[1] J. Łukasik,[2,3] W. F. J. Müller,[2] H. Orth,[2] C. Schwarz,[2] C. Sfienti,[2] W. Trautmann,[2] K. Turzó,[2] B. Zwiegliński,[4] A. Chbihi,[5] J. D. Frankland,[5] J. P. Wieleczko,[5] and M. Vigilante[6]
(ALADIN and INDRA@GSI Collaboration)
[1]*SUBATECH, Laboratoire de Physique Subatomique et des Technologies Associées, Université de Nantes - IN2P3/CNRS - EMN 4 rue Alfred Kastler, F-44072 Nantes, France*
[2]*GSI Helmholtzzentrum für Schwerionenforschung GmbH, D-64291 Darmstadt, Germany*
[3]*H. Niewodniczański Institute of Nuclear Physics, PL-31342 Kraków, Poland*
[4]*A. Sołtan Institute for Nuclear Studies, PL-00681 Warsaw, Poland*
[5]*GANIL, CEA, IN2P3-CNRS, B.P. 5027, F-14021 Caen Cedex, France*
[6]*Dipartimento di Scienze Fisiche, Università di Napoli, I-180126 Napoli, Italy*
(Received 9 June 2009; published 27 October 2009)

Recently, it has been observed that events with the *same* total transverse energy of light charged particles (LCP) in the quasitarget region, $E_{\perp 12}^{\mathrm{QT}}$, show two quite distinct reaction scenarios in the projectile domain: multifragmentation and residue production. This phenomenon has been dubbed "bimodality." Using quantum molecular dynamics calculations we demonstrate that this observation is very general. It appears in collisions of all symmetric systems larger than Ca and at beam energies between 50A MeV and 600A MeV and is due to large fluctuations of the impact parameter for a given $E_{\perp 12}^{\mathrm{QT}}$. Investigating in detail the $E_{\perp 12}^{\mathrm{QT}}$ bin in which both scenarios are present, we find that neither the average fragment momenta nor the average transverse and longitudinal energies of fragments show the behavior expected from a system in statistical equilibrium, in experiment as well as in QMD simulations. On the contrary, the experimental as well as the theoretical results point toward a fast process. This observation questions the conjecture that the observed bimodality is due to the coexistence of two phases at a given temperature in finite systems.

DOI: 10.1103/PhysRevC.80.044615 PACS number(s): 24.10.Lx, 24.60.Lz, 25.70.Pq

I. INTRODUCTION

A while ago the INDRA and ALADIN collaboration discovered [1] that, in collisions of heavy ions—Xe + Sn and Au + Au between 60 and 100 A MeV incident energy—in a small interval of the total transverse energy of light charged particles ($Z \leqslant 2$) in the quasitarget (QT) domain, $E_{\perp 12}^{\mathrm{QT}}$, a quantity which is usually considered as a good measure of the centrality of the reaction, two distinct reaction scenarios exist. In this $E_{\perp 12}^{\mathrm{QT}}$ interval, in the forward, quasiprojectile direction, either a heavy residue is formed which emits essentially light charged particles, or the system fragments into several intermediate mass fragments. In the original publication this phenomenon has been termed "bimodality" due to reasons we will discuss later on. We stick to this name although our interpretation of the origin of this phenomenon is different, and we will call this interval in $E_{\perp 12}^{\mathrm{QT}}$ "bimodality interval." In the meantime, this effect has also been observed by other groups [2].

This observation created a lot of attention due to the fact that a couple of years before a theory was launched which predicted that in finite size systems [3–5], in finite size systems a first order phase transition weakens: in a finite size canonical ensemble, which is determined by the temperature T, the number of particles N, and a given volume V (or a given pressure p), it becomes more like a crossover. In infinite matter the two phases coexist only at the transition temperature. Below the transition temperature, $T_t(N, V)$, the system is in one phase and above T_t in the other phase. Because energy fluctuations are suppressed by $\propto 1/\sqrt{N}$, this statement is also true if the large system is treated microcanonically. In finite systems, the situation is different. In a canonical description of the system, for a given T, N, and V, the energy fluctuations can become large, even larger than the finite latent heat. Therefore—for a given temperature close to T_t—for the same values of T, N, and V, the system can either be in the gas or in the liquid phase. This means that if the system stays in thermal equilibrium for long, it moves back and forth from one phase to the other. The simultaneous appearance of these two modes (phases) for a given value of T, N, V has been called "bimodality." In a microcanonical description, bimodality is not possible, because the energy of the two phases differs.

It is of course all but easy to identify these theoretical results with observables obtained in a heavy-ion reaction. Assuming that $E_{\perp 12}^{\mathrm{QT}}$ is also a measure of the temperature of the system [1], it is nevertheless tempting to identify the residue with the liquid phase of nuclear matter, and the creation of several medium or small size fragments with the gas phase. The experimental observation of the above-mentioned bimodality scenario would then just be the experimental confirmation of the theoretically predicted bimodality.

If this were true, the observation of bimodality would solve a longstanding problem of heavy-ion physics, the quest to identify the reaction mechanism which leads to multifragmentation. This problem arrived because many observables could be equally well described in thermodynamical or statistical theories [6,7] as in molecular dynamics type models [8–11], although the underlying reaction mechanism is quite different. The statistical models assume that the system is in statistical equilibrium when its density reaches a fraction of normal

 ©2009 The American Physical Society

nuclear matter density. Then, it suddenly freezes out and the fragment distribution is determined by phase space at freeze-out. In dynamical models, on the contrary, fragments are surviving initial state correlations which have not been destroyed by hard nucleon-nucleon collisions during the reaction, and equilibrium is not established during the reaction. They can be already identified very early in the reaction, when the density is still close to nuclear matter density. A detailed discussion of how the reaction proceeds in these models can be found in [12].

Recently, it has been shown that the observation of bimodality alone does not allow for the identification of the reaction mechanism. Dynamical models describe the bimodality signal as well. In the bimodality $E_{\perp 12}^{\mathrm{QT}}$ interval, they also show the presence of two different event classes, and reproduce quantitatively the scaling properties of $E_{\perp 12}^{\mathrm{QT}}$ [13]. Therefore, further studies of the bimodality interval in $E_{\perp 12}^{\mathrm{QT}}$ are necessary to elucidate the reaction mechanism.

The variables T, N, and V determine the canonical ensemble completely. If bimodality, in the sense of the coexistence of the two phases at a given temperature, is at the origin of the experimental observation, the values of the average source velocity of both modes as well as their temperature have to be identical.

In this article, we analyze the experimental and theoretical events which fall in the bimodality $E_{\perp 12}^{\mathrm{QT}}$ interval, without further cuts, to study the average system properties in this interval, and to investigate why bimodality, defined as above as the observation of two different reaction scenarios in a narrow interval of $E_{\perp 12}^{\mathrm{QT}}$, is feasible even if the system has not reached thermal equilibrium. In Sec. II, we investigate in detail the experimental observables in the bimodality $E_{\perp 12}^{\mathrm{QT}}$ bin and whether they are compatible with the assumption that there are two phases in thermal equilibrium. This detailed study is possible due to the very good acceptance properties of the INDRA detector. In a second step, we investigate in Sec. III whether bimodality is a phenomenon which occurs only in a small range of system sizes and beam energies in which the system hits the transition temperature, or whether it is a more general phenomenon. Especially, the energy dependence is of interest, because with increasing energy there is a change in the type of matter from which fragments are formed. At low energies, it is the participant matter (the overlapping part of projectile and target) which forms the fragments, whereas at energies of a couple of hundred A MeV, the fragments are formed from spectator matter (the nonoverlapping part) [12,15].

II. SYSTEM PROPERTIES IN THE BIMODALITY INTERVAL OF $E_{\perp 12}^{\mathrm{QT}}$

For the investigation of the physics in the bimodality $E_{\perp 12}^{\mathrm{QT}}$ interval, we follow the definitions of Ref. [1]. $E_{\perp 12}^{\mathrm{QT}}$ is defined as the total transverse energy of particles with charge $Z \leqslant 2$ on the quasitarget side ($\theta_{\mathrm{c.m.}} \geqslant 90^{\circ}$), calculated in the frame in which the momentum tensor of all fragments with charge $Z \geqslant 3$ is diagonal. The diagonalization is done event by event.

We define a_2 as

$$a_2 = (Z_{\mathrm{max1}} - Z_{\mathrm{max2}})/(Z_{\mathrm{max1}} + Z_{\mathrm{max2}}), \tag{1}$$

where Z_{max1} is the charge of the largest fragment, while Z_{max2} is the charge of the second largest fragment, both observed in the same event in the quasiprojectile (QP) hemisphere—at polar angles $\theta_{\mathrm{c.m.}} < 90^{\circ}$—in the center of mass of the system. For a more accurate extraction of a_2, we reject events where less than 70% of the charge of the projectile has been detected. Bimodality means that there exists a narrow interval in $E_{\perp 12}^{\mathrm{QT}}$ in which events with large and small a_2 values are observed. In this narrow transition region, we expect two types of events: One with one big projectile residue accompanied with some very light fragments (large a_2), and the other with two or more similarly sized fragments (small a_2). Events with intermediate values of a_2 should be rare. In [13] we have studied a_2 as a function of $E_{\perp 12}^{\mathrm{QT}}$ for the system Au + Au between 60A MeV and 150A MeV incident energy that has been measured by the INDRA-ALADIN collaboration at GSI [14]. We focus here on the data at 60A MeV and concentrate on that experimental bimodality interval of $E_{\perp 12}^{\mathrm{QT}}$ where the transition from small to large a_2 values occurs. We compare the experimental events in this interval with filtered numerical simulations for the same $E_{\perp 12}^{\mathrm{QT}}$ values. The filtering is done using a software replica of the INDRA experimental setup.

The simulations are performed with one of the dynamical models which has frequently been used to interpret the multifragmentation observables, the quantum molecular dynamics (QMD) approach [8,9,12]. This approach simulates the entire heavy-ion reaction, from the initial approach of projectile and target up to the final state, composed of fragments and single nucleons. Here, nucleons interact by mutual density-dependent two-body interactions and by collisions. The two-body interaction is a parametrization of the Brückner G-matrix supplemented by an effective Coulomb interaction. For this work, we have used a soft equation of state. The initial positions and momenta of the nucleons are randomly chosen and respect the measured rms radius of the nuclei as well as the Fermi distribution in momentum space. Collisions take place if two nucleons come closer than $r = \sqrt{\sigma/\pi}$, where σ is the energy-dependent cross section for the corresponding channel (pp or pn). The scattering angle is chosen randomly, respecting the experimentally measured $d\sigma/d\Omega$. Collisions may be Pauli blocked. For details we refer to Refs. [8,9]. For the later discussion, it is important to note that, even for a given impact parameter, two simulations are not identical, because the initial positions and momenta of the nucleons as well as the scattering angles are randomly chosen. It has been shown [13] that these simulations give a bimodality signal in the same $E_{\perp 12}^{\mathrm{QT}}$ bin as the experiment and that the beam energy dependence of this transition is reproduced.

A. a_2 dependence of observables

If the experimental signal, i.e., the existence of two distinct reaction scenarios in a certain $E_{\perp 12}^{\mathrm{QT}}$ interval, reflects the coexistence of two phases of a thermally equilibrated system, the behavior of several observables can be predicted. In this case,

both phases must have the same source velocity in the c.m. and the same temperature. Considering the nuclei resulting from the decay of the projectile spectator as an ideal, classical, noninteracting gas, the mean kinetic energy of each fragment or nucleon in the center-of-mass frame of this gas should be $3kT/2$. This has also to be true for the largest fragment, called the projectile remnant (PR), in contradistinction to other theoretical approaches in which the PR properties reflect the violence of the reaction, which depends on centrality and hence on its size. The longitudinal velocity loss and the transverse velocity of the heaviest fragment have been systematically studied for different projectile-target combinations [16]. The value of both differs from the expectation for a heat bath particle, and depends on the number of nucleons the projectile has lost in the course of the interaction. This is one of the interests to study first for the properties of $Z_{\max 1}$ in the bimodality $E^{\mathrm{QT}}_{\perp 12}$ interval. The other is that observables of the heaviest fragment should give a clear signal of the process because they are the least spoiled by eventual pre-equilibrium processes which may disturb the light particle spectra. Figure 1 shows the transverse velocity $\beta_\perp = v_\perp/c$ (top) and the longitudinal velocity, $\beta_\parallel = v_\parallel/c$ (middle), in the c.m. of the system, for the heaviest fragment in the QP region as a function a_2 and for those fragments which belong to events which fall into the bimodality interval, $12 < E^{\mathrm{QT}}_{\perp\,12}/E_{0\mathrm{c.m.}} < 17$. $E_{0\mathrm{c.m.}}$ is the incident energy per nucleon in the c.m. system. The bottom panel displays the average charge of the heaviest fragment as a function of a_2. In all figures, we show the INDRA data as points and compare the experimental results with unfiltered (full line) and filtered (dashed line) QMD predictions. We see that the filter changes substantially $\beta_\perp$ (due to a cutoff at small transverse velocities) and to a less extent $\beta_\parallel$. After filtering, the QMD calculations reproduce the trend of the data but overpredict the transparency, i.e., underpredicts $\beta_\perp$, for small a_2 events corresponding to those with a small $Z_{\max 1}$. If our assumption that $E^{\mathrm{QT}}_{\perp 12}$ characterizes the excitation energy and hence the temperature of the system and that the events in the bimodality bin have that temperature at which the system can either be in the gas or in the liquid phase, we expect that $\beta_\perp$ as well as $\beta_\parallel - \beta_{\mathrm{source}} \propto 1/\sqrt{\mathrm{mass}}$. Here β_{source} is the velocity of the bimodal system in the c.m. which should be independent of a_2 because the velocity of the bimodal system does not depend on which mode is realized.

Consequently, this assumption does not offer the possibility that $\beta_\parallel$ increases with the particle mass or charge. The experimentally observed linear increase of $\beta_\parallel$ with the mass of the fragment follows, however, the trend already observed in central and semicentral Xe + Sn events at 100A MeV [19] (where no bimodality has been observed). The average velocity of the heaviest fragment, in events with a smaller $E^{\mathrm{QT}}_{\perp 12}$ than at bimodality, follows this systematics as well. This linear decrease of the PR velocity with decreasing mass is a very general phenomenon which was first studied by Morrissey [16] and complemented for higher-beam energies by Ricciardi *et al.* [17], although it has not been shown yet that this systematics is still valid for such small PR in this energy domain. Such a linear dependence is expected if nucleons are removed randomly from the cold projectile nucleus, under the condition that they do not interact with the residue anymore. This removal leads to a deceleration and an excitation of the remnant. Thus this increase of $\beta_\parallel$ can be understood in models in which the heaviest fragment is not in thermal equilibrium with the emitted particles, but finds no explanation in purely thermal models.

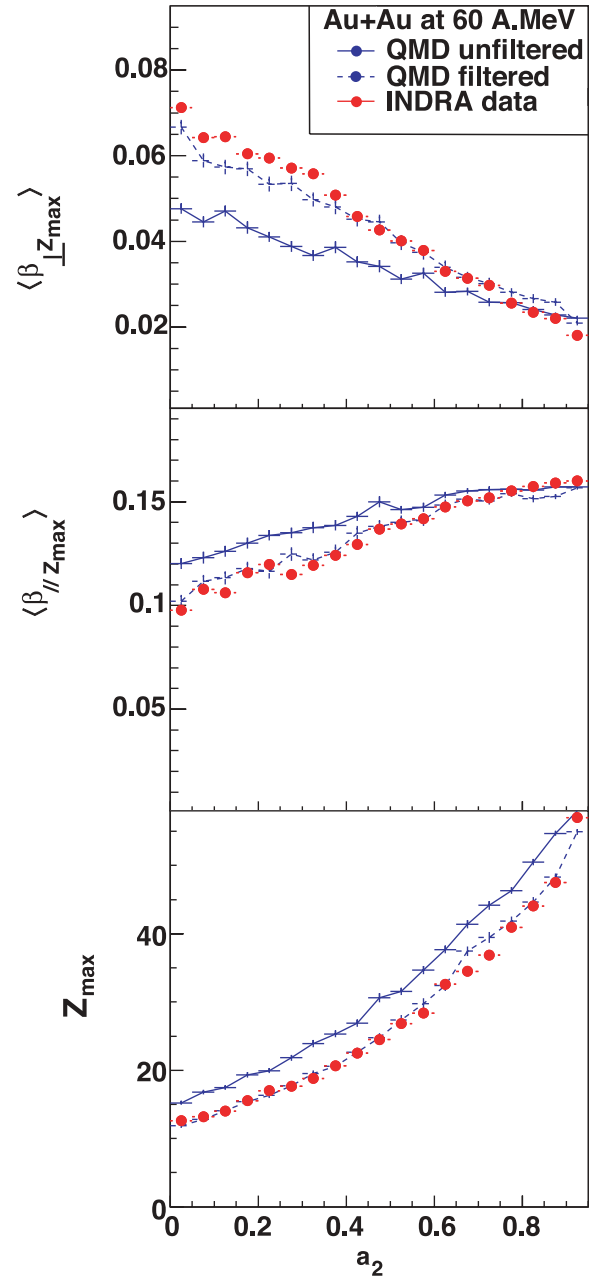

FIG. 1. (Color online) Average transverse velocity $\beta_\perp = v_\perp/c$ (top) and $\beta_\parallel = v_\parallel/c$ (middle) of the QP fragment ($\theta_{\mathrm{c.m.}} < 90^\circ$) with the largest charge, $Z_{\max 1}$, as well as $Z_{\max 1}$ (bottom) as a function of the QP a_2 for those events which fall in the bimodality interval $E^{\mathrm{QT}}_{\perp 12}$, see text. We compare INDRA data (symbols) with filtered (dashed lines) and unfiltered (full lines) QMD simulations for Au + Au collisions at 60A MeV bombarding energy.

In addition, we observe that the average transverse velocity decreases with a_2. In order to discuss the compatibility with

the assumption of a canonical bimodal system, we have to consider the unfiltered QMD events. They show an almost constant transverse kinetic energy of 35 MeV, independent of the fragment mass and charge, as will be discussed at the end of Sec. II B. This value confirms the analysis of [18] and is too large (even if one considers a radial flow, as we discuss in the next section) to be compatible with kT: the expected kinetic energy for fragments in a thermal heat bath has to be smaller than the binding energy of nucleons. Hence, in the bimodality $E^{\rm QT}_{\perp 12}$interval, also $\beta_\perp$ is also incompatible with the assumptions that two phases are present, both having the same temperature.

Thus neither the mass dependence of $\beta_\parallel$ nor that of $\beta_\parallel$ of the heaviest fragment $Z_{\rm max1}$ in the bimodality $E^{\rm QT}_{\perp 12}$ interval are compatible with the expectations for a finite system in which two phases are in equilibrium. On the contrary, they follow the systematics which we have observed for other $E^{\rm QT}_{\perp 12}$ regions where no experimental signs of the presence of two phases in thermal equilibrium, i.e., bimodality behavior, are found. These properties can be explained in models which are genuinely nonequilibrium and which have successfully been applied to interpret data in many experimental situations.

B. Particle properties in the $E^{\rm QT}_{\perp 12}$ interval which shows bimodality

A thermal system has to be isotropic in its rest system. The system we study here is the ensemble of all QP particles, i.e., those which are emitted at angles $\theta_{\rm c.m.} < 90^\circ$. The degree of isotropy can be studied with the help of the momentum tensor in the rest system of the source

$$Q_{zz} = \frac{2\langle p_z^2\rangle - \langle p_y^2\rangle - \langle p_x^2\rangle}{\langle p^2\rangle}. \tag{2}$$

p_z is the momentum in the beam direction. $Q_{zz} = 0$ if in the rest system of the source the distribution is isotropic. Negative values indicate a preferred emission in transverse direction. Figure 2 gives an overview over Q_{zz} of light charged particles ($Z = 1, 2$) and fragments ($Z \geqslant 3$) in the bimodality $E^{\rm QT}_{\perp 12}$ interval.

The average longitudinal velocity of all quasiprojectile nucleons in the c.m. depends on a_2. In the bimodality scenario this should not be the case. It is therefore not meaningful to analyze all events of the bimodality $E^{\rm QT}_{\perp 12}$ interval in a common rest frame. We concentrate here on the question of whether for a given a_2 the events are isotropic. This a necessary but—as just mentioned—not a sufficient condition for bimodality. To obtain the Q_{zz} distribution, we adopt the following procedure: We select events which fall into the $E^{\rm QT}_{\perp 12}$ interval which shows bimodality and calculate for each a_2 bin the average velocity of a) all LCP ($Z = 1, 2$) and b) of all fragments $Z \geqslant 3$ of all events which fall in this bin. In one of the rest systems we calculate subsequently for each event Q_{zz} of either the fragments or the LCP. This procedure is applied to eliminate the dependence of the velocity of the rest system of the fragments on a_2 (see Fig. 1), because we expect isotropy only in the rest system. From top to bottom,

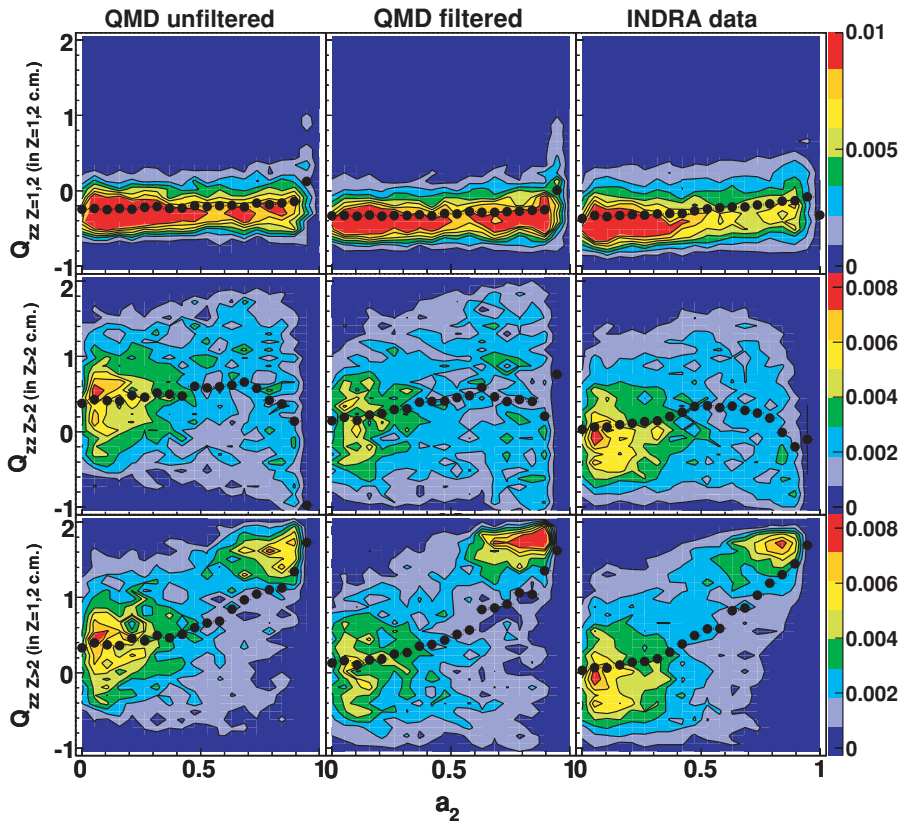

FIG. 2. (Color online) Distribution of Q_{zz} for Au + Au events at 60A MeV which fall in the $E^{\rm QT}_{\perp 12}$ bimodality bin. We display the Q_{zz} distribution (see text) for light charged particles ($Z = 1, 2$) (top row) in their own center of mass, and for fragments with charge $Z \geqslant 3$ in their own (middle row) and in the $Z = 1, 2$ c.m. system (bottom row), as a function of a_2. The points are the mean values of Q_{zz} as a function of a_2. From left to right, we display unfiltered and filtered QMD predictions, and the INDRA data, respectively. The points mark the mean values.

we display the Q_{zz} distribution of the LCP in the rest system of the LCP, that of fragments in the rest system of the fragments, and that of fragments in the rest system of the LCP. From left to right we show the unfiltered, the filtered QMD predictions, and the INDRA data, respectively. Please note that the $E_{\perp 12}^{\mathrm{QT}}$ interval is determined by the energy of the $Z = 1, 2$ particles in the QT domain, whereas here we study the properties of $Z = 1, 2$ particles in the QP domain. Thus, autocorrelations between $E_{\perp 12}^{\mathrm{QT}}$ and the particles studied in the QP domain are minimized.

We see from the top figures that the LCP in this $E_{\perp 12}^{\mathrm{QT}}$ interval are preferably emitted into a transverse direction in their rest frame ($Q_{zz} < 0$). The anisotropy depends only slightly on a_2. It may be due to the fact that not only the bimodal system but also pre-equilibrium emission contributes to the spectra. It indicates that the origin of the $Z = 1, 2$ is never a pure thermal source, neither for small a_2 nor for large a_2 events. The experimental filter changes little as far as the LCP anisotropy is concerned and the filtered QMD predictions agree quite well with the INDRA data. In their proper rest system the fragments are emitted preferably in the forward/backward direction. The experimental filter brings the QMD predictions of the average Q_{zz} value closer to zero, in agrement with the experiment. At very large values of a_2, the emission becomes isotropic. Such an isotropy is expected, for example, for the emission of a light charged fragment from a compound nucleus. For small a_2 values, Q_{zz} of the fragments in the rest system of the LCP fluctuates around zero as expected for an isotropic source. Thus small a_2 events come closest to isotropy. For $a_2 > 0.5$, Q_{zz} is close to 2. This means that in the LCP rest system, the largest fragment is preferably emitted in the beam direction. This observation rules out, on the other hand, the hypothesis that the ensemble of fragments and light charged particles at large a_2 values can be considered as a pure liquid phase. This would require that the direction of the velocity of the largest fragment is randomly distributed in the rest system of the liquid.

One may argue that the largest fragment is not really in thermal equilibrium in the sense that it has not lost completely its memory on the entrance channel, i.e., its initial velocity direction. Such an argument cannot be put forward for the second largest fragment. Therefore, we display in Fig. 3 the average Q_{zz} for the second largest fragments calculated in the rest system of those fragments. The INDRA data (symbols) as well as the unfiltered (full line) and filtered (dashed line) QMD events show $Q_{zz} \leqslant 0$ independent of a_2. The value of $Q_{zz} \approx -0.2$ for large a_2 indicates that the emission of the second largest fragment is essentially random but still more probable in transverse direction in the fragment rest system. For the small a_2 values we find $Q_{zz} \approx -0.4$. Again, the second largest fragment is preferably emitted in the transverse direction. For the interpretation, we have to combine this result with that shown in the lower right panel of Fig. 2: In the rest system of the fragment, the emission of *all* fragments is almost isotropic. A small value of a_2 means that the two biggest fragments have about the same size. Therefore, combining the Q_{zz} of all fragments and of the second largest fragments yields the following scenario: For small a_2 values the fragment

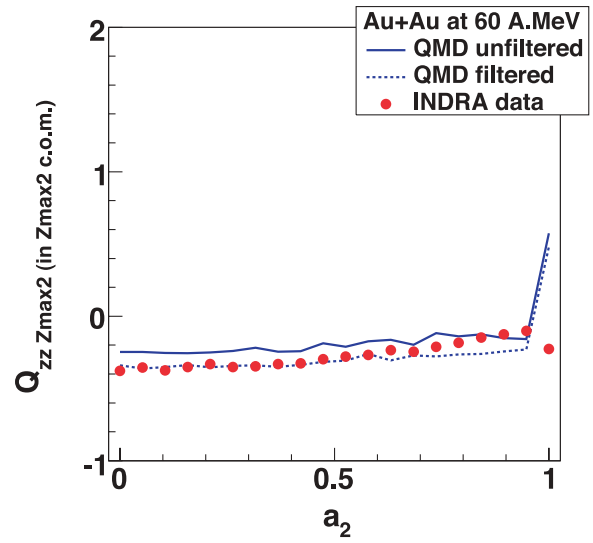

FIG. 3. (Color online) Q_{zz} for Au + Au at 60A MeV in the $E_{\perp 12}^{\mathrm{QT}}$ bimodality bin calculated for the second largest charges Z_{max2} of all events taken all together (around their average momentum), as a function of a_2. We compare INDRA data (symbols) with filtered (dashed lines) and unfiltered (full lines) QMD predictions for Au + Au collisions at 60A MeV.

with the highest charge has the largest velocity in the beam direction, but this time the lighter fragment can balance the momentum and therefore the total emission pattern *appears* to be isotropic, although, if one looks into the detail, it is not.

Thus, only for the largest a_2 values, the fragments are isotropically distributed in their rest system as they should be if the QP system represents the vapor or the liquid phase of a system in thermal equilibrium. This observation for large a_2 values is also compatible with the emission of a light fragment from a compound nucleus.

Figure 4 shows the average velocity in longitudinal $\beta_{\parallel \mathrm{c.m.}}$ and transverse direction $\beta_{\perp}$ in the reaction c.m. system as a function of the fragment mass, for those events which fall in the bimodality interval of $E_{\perp 12}^{\mathrm{QT}}$ (left) and for all events (right). In all figures we display the INDRA data as points and compare them to the unfiltered (full line) and filtered (dashed line) QMD predictions. Similar to Fig. 1, we observe also here an increase of $\beta_{\parallel}$ with increasing fragment mass. For large fragments the velocity approaches that of the beam ($\beta_{\parallel} = 0.179$). The fragments in the selected $E_{\perp 12}^{\mathrm{QT}}$ bin show—as Z_{max1}—an almost identical behavior to those observed without a selection in $E_{\perp 12}^{\mathrm{QT}}$, and follow the Morrissey systematics [16]. QMD simulations reproduce $\beta_{\parallel}$ rather well. The transverse velocity of the heavy fragments is small and increases with decreasing fragment mass. Such a dependence has been observed for systems with a collective radial velocity [28]. In such a scenario, the form of the velocity dependence of the mass allows for the determination of the temperature and of the radial velocity if the emitting source is thermal with a collective radial velocity [28]. In a thermal system, $E_{\perp} = kT$. The dotted curve, calculated according to the formula given in Ref. [28], gives the best agreement with the experimental data for $E_{\perp} = 13.5$ MeV. This value is too

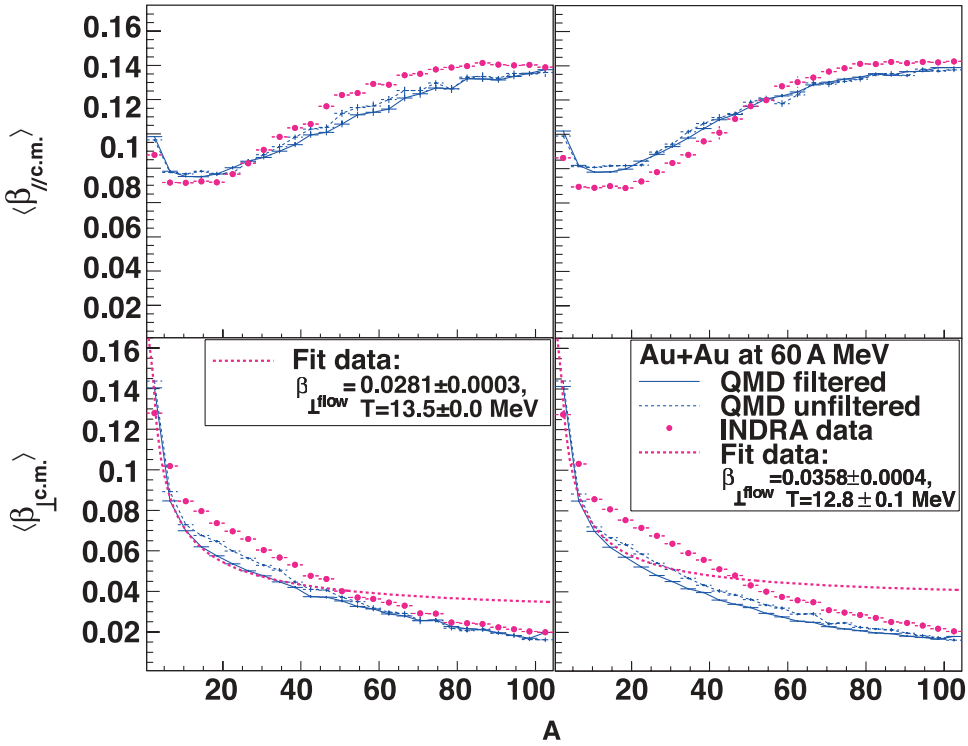

FIG. 4. (Color online) Average longitudinal $\langle\beta_\parallel\rangle$ and average transverse velocity $\langle\beta_\perp\rangle$ in the reaction center of mass system as a function of the fragment mass. In the left panels, we display the quantities for those fragments which belong to events in the bimodality interval of $E^{\rm QT}_{\perp 12}$, and in the right panels for those of all events without any $E^{\rm QT}_{\perp 12}$ cut. INDRA data (symbols) are compared with filtered (dashed lines) and unfiltered (solid lines) QMD predictions for Au + Au collisions at 60A MeV. The dashed bold line is the result of the fit of the experimental data, using the approach of Ref. [28]

high to be compatible with the assumption of a thermalized system. At such a temperature, the fragments would not exist anymore.

On the contrary, the observed value of 13.5 MeV is well described by the Goldhaber model [16,22]. It is based on the assumption that nucleons or fragments are removed rapidly from a *cold* nucleus and therefore their momentum distribution is given by the Fermi motion. Then, the average transverse squared momentum per nucleon of a fragment of size A_F is given by the Goldhaber formula [22]:

$$p_\perp^2(A_F) \approx \frac{2}{3}\cdot\frac{3}{5}p_F^2 A_F \frac{A_P - A_F}{A_P - 1}, \tag{3}$$

where $A_P(A_P)$ is the projectile (fragment) mass and p_F denotes the Fermi momentum. Therefore

$$E_\perp(A_F) = \frac{p_\perp^2(A_F)}{2A_F m_N} \approx \frac{1}{5}\frac{p_F^2}{m_N} \approx 14\ \text{MeV} \tag{4}$$

is almost independent of the fragment size and in agreement with the data. The QMD simulations reproduce the form and the absolute value of $\beta_\perp(A)$. This is not astonishing, because, in this model, fragments are surviving initial correlations which preserve approximately the transverse momentum they had initially, and therefore, the average transverse energies of intermediate mass fragments are, independent of the impact parameter, close to the value expected from the Goldhaber formula. Thus, the fragment average transverse velocities are understandable if one assumes that there is a collective radial expansion of the system which is superimposed to an average transverse energy given by the Goldhaber model.

Figure 5 displays the experimental average transverse energy, $E_\perp$, as a function of the fragment mass of QP products. We see indeed that $E_\perp$ in unfiltered QMD predictions is almost independent of the fragment size. Filtering for the experimental acceptance increases $E_\perp$ for intermediate mass fragments and brings the calculation closer to the experimental observation. $E_\parallel$, on the contrary, is strongly mass dependent in the rest system of the QP. Up to $A = 50$, this dependence is well reproduced by QMD predictions. Above, there are discrepancies.

A thermal system has to be isotropic in coordinate and momentum space, and for each degree of freedom, the average kinetic energy of the fragments has to be $E = \frac{1}{2}kT$ in the rest system of the source. Therefore it is meaningful to calculate the deviation of

$$R = \frac{\langle\beta_\perp^2\rangle}{2\langle(\beta_\parallel - \langle\beta_\parallel\rangle)^2\rangle} \tag{5}$$

from 1. The INDRA data as well as the QMD predictions, displayed in Fig. 5, show that R strongly depends on the fragment size. Up to mass $A = 40$, R decreases strongly and increases slightly at higher masses. Therefore, this specific bimodality $E^{\rm QT}_{\perp 12}$ interval shows the same behavior which has been observed in [23] for central collisions, where bimodality does not occur. The discrepancy above $A = 40$ between the experimental data and the QMD predictions disappears if one rejects the symmetric and asymmetric fission events (by requiring that the product of the two largest charges is smaller than 600). Thus, these deviations come from events in which two fragments of similar charge are observed.

III. SYSTEM SIZE DEPENDENCE OF BIMODALITY

After having established that most of the data for Au + Au collisions at 60A MeV are quantitatively described in QMD calculations, we study now the system size dependence of the bimodality. Unfortunately, no data have been published so far to verify these theoretical predictions. In order to discuss

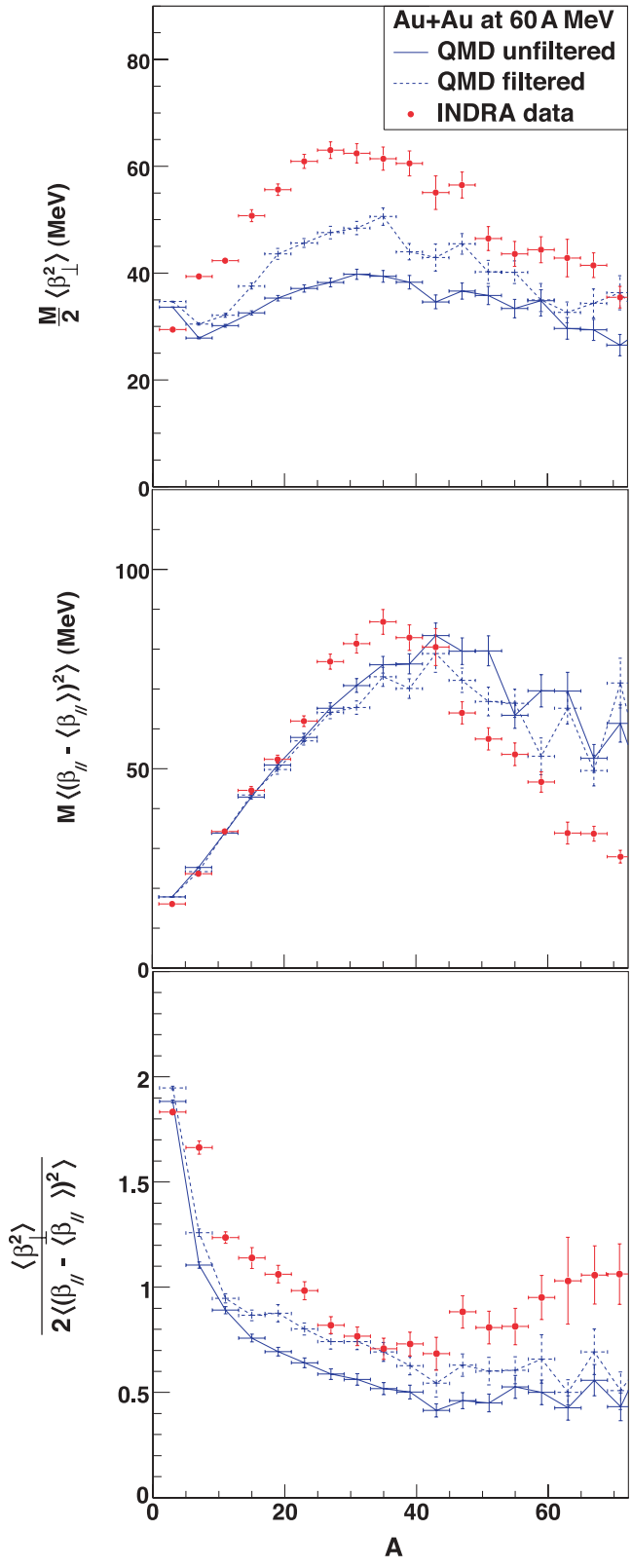

FIG. 5. (Color online) Twice the average longitudinal (top right) and the transverse (top left) kinetic energy of QP products in the QP center of mass system, as well as the ratio of both (bottom), as a function of their mass. We compare the INDRA data with filtered (dashed lines) and unfiltered (full lines) QMD predictions for Au + Au collisions at 60A MeV in the bimodality $E_{\perp 12}^{\mathrm{QT}}$ region.

the physics, we present, in Fig. 6, a_2 as a function of the reduced $E_{\perp 12}$ (right) as well as a function of the reduced impact parameter b/b_0 (left). Here, $E_{\perp 12}$ is calculated over all particles with charge $Z = 1, 2$ (QT and QP) and a_2 is given for QP products. To account for system energy and size scalings, $E_{\perp 12}$ is divided by the total mass of the system and by the energy per nucleon in the center of mass. The top row shows a_2 calculated with all fragments. For the bottom row, we require that the fragment with the largest charge, Z_{max1}, and that with the second largest charge Z_{max2} have both a charge larger than 2. We start the discussion with the Au + Au reaction (top left) for which we zoom on the narrow impact parameter interval 5 fm $\leqslant b \leqslant$ 7 fm, where bimodality occurs. If plotted as a function of $E_{\perp 12}$ for this impact parameter interval, we clearly see the two event classes with a distinct a_2 value for the same small $E_{\perp 12}$ interval. Whether we limit the events to $Z_{\mathrm{max1}} > 2$ and $Z_{\mathrm{max2}} > 2$ or not does not make a difference, because there are almost always two fragments with $Z \geqslant 3$. When plotted as a function of b/b_0, the bimodality structure with a sudden jump disappears. There, the events with a small a_2 value are distributed over a broad range of impact parameters [12]. Because the fluctuations in $E_{\perp 12}$ for a given impact parameter are large, some of these events appear in the same bimodality interval in $E_{\perp 12}$ as the events with a large a_2. This is shown in Fig. 7 which displays the filtered INDRA $E_{\perp 12}$ distribution and that of b/b_0 for a given unfiltered $E_{\perp 12}$ in QMD simulations of Au + Au reactions at 60A MeV. For an incident energy of 100A MeV, the distributions are similar. The bars mark the standard deviation. We see that there is a strong correlation between these observables. In particular, the INDRA setup provides a mean linear response—no saturation—to $E_{\perp 12}$ over a large range of $E_{\perp 12}$ (hence to the multiplicity and to the energy of particles). The distributions are, however, quite broad, and hence, for a given experimentally measured $E_{\perp 12}$ value, the unfiltered $E_{\perp 12}$'s as well as the impact parameters show large fluctuations.

Like Au + Au, the smaller Xe + Sn system (Fig. 6, top right) exhibits two distinct maxima of a_2, with a sudden jump of the most probable value of a_2 (depicted by the dashed lines). The two event classes are also seen if the events are plotted as a function of b/b_0, and it is visible that they are both associated with quite different impact parameters. Thus, nuclei disintegrate in two quite distinct patterns, but they belong to quite different impact parameters, and, hence, to quite different reaction geometries. For the even smaller Kr + Kr system (Fig. 6, bottom left), there is still a sudden jump of a_2 as a function of $E_{\perp 12}$, but the two event classes become less distinct, the relative yield of intermediate a_2 values getting higher. This can be explained by the fact that the absolute value of $E_{\perp 12}$ is reduced and hence the relative fluctuations around the mean value increase for a given b/b_0. Therefore, we find again the existence of the two maxima in a_2 for (almost) the same value of the reduced $E_{\perp 12}$ if $Z_{\mathrm{max1}} > 2$ and $Z_{\mathrm{max2}} > 2$. The impact parameter of the two event classes is, however, quite different, the minimum of a_2 is less pronounced. In addition, events with $Z_{\mathrm{max1}} > 2$ and $Z_{\mathrm{max2}} > 2$ become rare. The majority of events with a large a_2 value are now those in which the second largest fragment charge has $Z = 2$. For such small systems, already a beam energy of 100A MeV

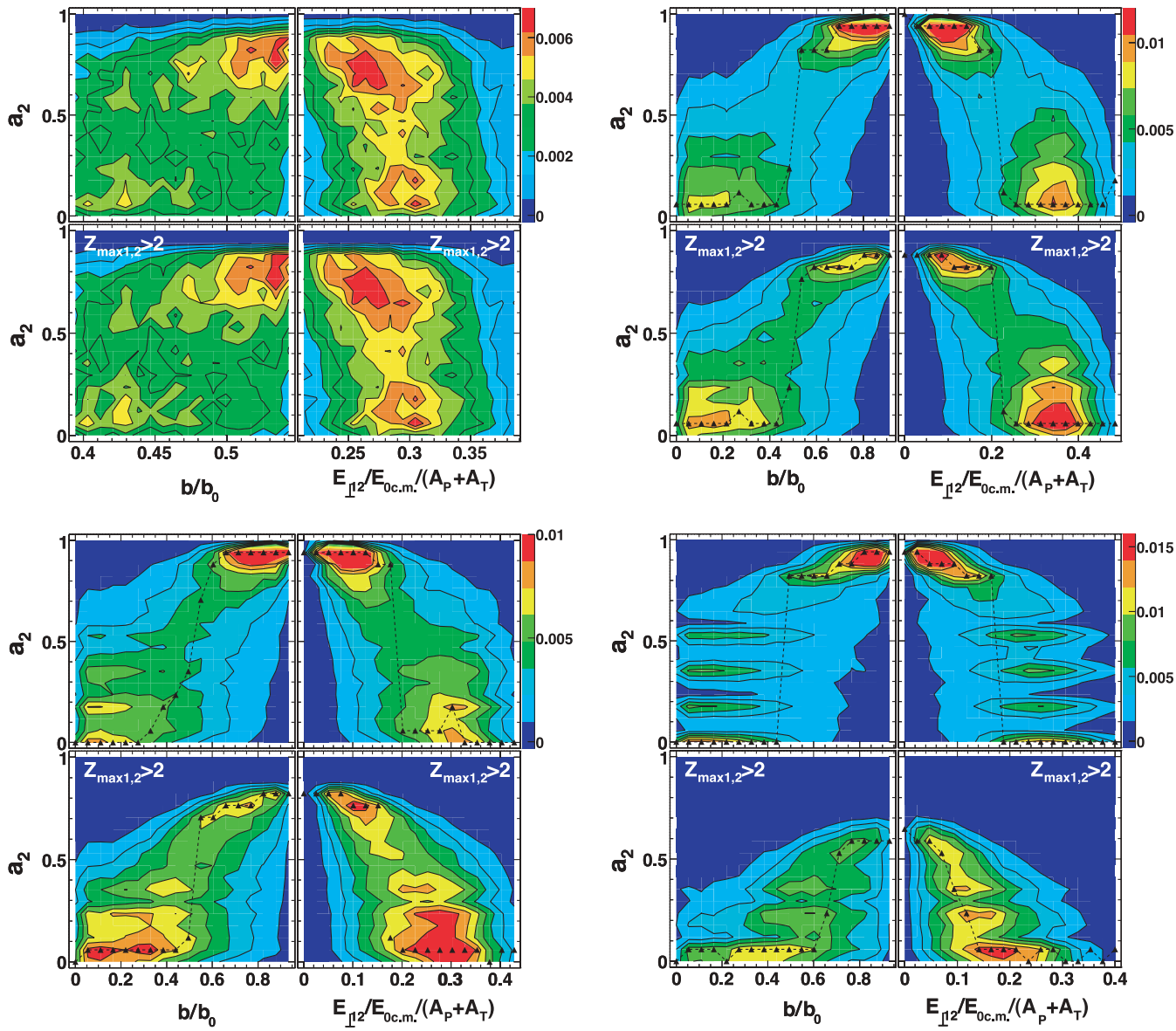

FIG. 6. (Color online) Double differential reaction cross section (linear color scale normalized to the number of events) as a function of a_2 and of the reduced impact parameter b/b_0 and the reduced $E_{\perp 12}$ (see text), respectively. The symbols show the most probable values of a_2. The dotted line is to guide the eye. In the top row of each panel, all events are accepted, in the bottom row only those with $Z_{\mathrm{max1}} > 2$ and $Z_{\mathrm{max2}} > 2$ are shown. We display Au + Au (top left), Xe + Sn (top right), Kr + Kr (bottom left), and Ca + Ca (bottom right) reactions at 100A MeV incident energy. For Au + Au, note that a narrow selection in impact parameter (5 fm $\leqslant b \leqslant$ 7 fm) has been applied around the bimodality region.

makes the reaction that much more violent that in central collisions fragments hardly survive. Finally, for the very small system Ca + Ca (Fig. 6, bottom right), bimodality becomes almost impossible, many intermediate values of a_2 are highly populated, because the system is too small. For the rare events with $Z_{\mathrm{max1}} > 2$ and $Z_{\mathrm{max2}} > 2$, large values of a_2 are impossible, and therefore we cannot have two distinct maxima anymore. The reaction is dominated by α emission from the QP, as can be seen in the top row.

It is remarkable that, independent of the system size, the sudden jump of the mean a_2 value occurs around $E_{\perp 12}/E_{0\mathrm{c.m.}}/(A_P + A_T) \approx 0.2$, i.e., when the transverse energy of light charged particles per nucleon is identical. This scaling is understandable, because this quantity measures the energy transfer in the reaction and extends the scaling we have observed already for the beam-energy dependence of the bimodality for the Au + Au system [1,13].

It is an important observation that nature disfavors intermediate a_2 ($a_2 \approx 0.5$) values. Either a big cluster emits small fragments or we observe multifragmentation, events in which several intermediate mass fragments are produced. The dominance of these two reaction scenarios is independent of the system size. Dynamical models reproduce this observation but it is very desirable to know whether also statistical models

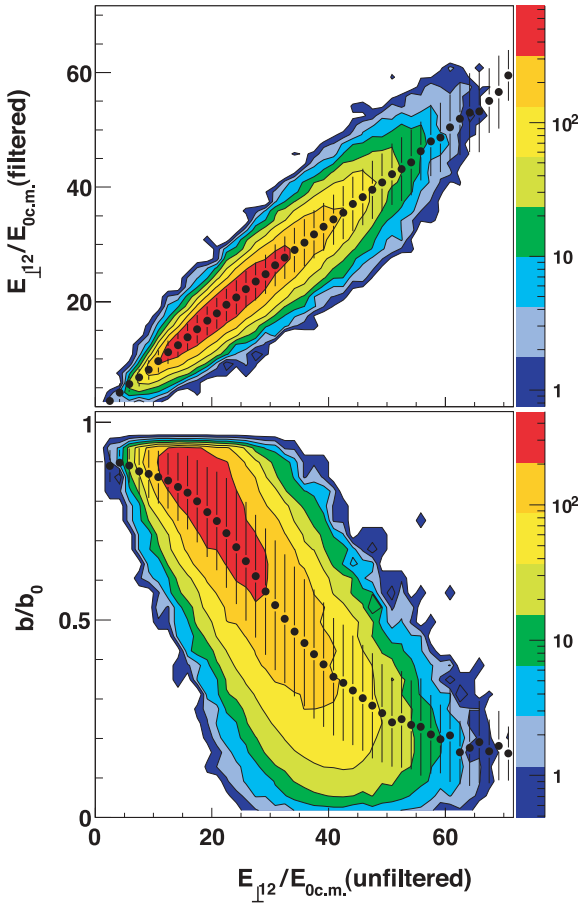

FIG. 7. (Color online) Double differential reaction cross section (logarithmic color scale in arbitrary units), for Au + Au at 60A MeV QMD predictions, as a function of $E_{\perp 12}$ divided by the kinetic energy per nucleon in the center of mass of the reaction system for INDRA filtered events (top) and as a function of the reduced impact parameter b/b_0 (bottom), respectively, and as a function of the unfiltered reduced $E_{\perp 12}$. The symbols show the mean values of $E_{\perp 12}/E_{0\text{c.m.}}$ and the error bars the rms of their distribution.

predict such a suppression of intermediate a_2 events. This would allow to elucidate whether this suppression is related to phase space or to the nucleon-nucleon interaction.

Independent of the system size, the events with large a_2 belong to other impact parameters than those with a small a_2. But $E_{\perp 12}$ and the impact parameter are not well correlated and therefore, due to the fluctuations of $E_{\perp 12}$ for a given impact parameter, events with very different a_2 values appear in the same $E_{\perp 12}$ interval. For smaller systems, the events with large a_2 are those in which an α particle is emitted from the residue. There we see as well that events with different a_2 do not belong to the same $E_{\perp 12}$ interval.

IV. ENERGY DEPENDENCE OF BIMODALITY

If bimodality is a special manifestation of the general feature that, in heavy-ion reactions, two distinct reaction scenarios with quite different a_2 values exist, it is tempting to see whether this observation continues to higher energies. Whereas at low energies multifragmentation happens in central collisions, and therefore fragments are formed from the participating nucleons, at higher energies [12], multifragmentation happens at large impact parameters and fragments are formed from spectator nucleons. There are not many experimental results available which allow to study this question, especially since there is no experiment in which simultaneously $E_{\perp 12}$ and all fragment charges have been measured in the target or projectile spectator. The only experiment which allows to address this question is the ALADIN experiment at GSI. In this experiment, Au + Au at 600A MeV incident energy [33], almost all fragments with $Z \geqslant 2$ of the projectile spectator (PS), i.e., in the forward direction, have been measured, but no light charged particles. Because $Z = 1$ particles are not measured, $E_{\perp 12}^{\text{PS}}$cannot be extracted, and we have to conclude the existence of bimodality indirectly. In Ref. [30], it has been shown, however, that the inclusive (impact parameter averaged) yield of a_2 has maxima at small and large values, separated by a minimum at around $a_2 = 0.5$, similar to the observations at energies around 100A MeV.

These data have also been analyzed by a statistical model approach [31] where it has been shown that the experimental mean values and fluctuations are well described once the distribution of the system energy, E, has been adapted. It has, however, not been demonstrated that this energy distribution corresponds to that which is expected for a given temperature of the system, as required by the bimodality assumption. In any case, the experimental inverse slope parameters are much larger than those of statistical model calculations [32]. These experimental parameters are compatible with the prediction of the Goldhaber model [Eq. (3)].

In a first step, we have to verify that QMD simulations reproduce correctly the pattern of a_2 as a function of Z_{bound}, the measured charge of all fragments with $2 \leqslant Z \leqslant 30$ (Z_{b2}) or $3 \leqslant Z \leqslant 30$ (Z_{b3}) in the PS. In the ALADIN experiments, it has been shown that Z_{bound} is strongly correlated with the energy deposit during the reaction [33]. In a second step, we replace then Z_{bound} by $E_{\perp 12}$ (calculated with both target and projectile spectator particles). Because Z_{bound} as well as $E_{\perp 12}$ are considered as a good measure for the centrality of the reaction, and more precisely of the energy deposit in the spectator, such a replacement is meaningful. Figure 8 shows in the two top rows a_2 as a function of the bound charge in the PS domain. On the left-hand side, we display the results obtained with the ALADIN setup, on the right-hand side the filtered QMD events. Filtering is not a very important issue here, because the ALADIN setup registers the large majority of the fragments in the PS region. a_2 as a function of Z_{b2} and Z_{b3} is shown in the top and middle panels, respectively. We see a quite reasonable agreement between theory and experiment. This allows us to replace in the bottom row Z_{bound} by $E_{\perp 12}$. On the right-hand side of the bottom row, we see that also at 600A MeV bimodality can be observed. In a $E_{\perp 12}$ interval around 9 GeV, we see two event classes: one with a large and one with a small value of a_2. The left-hand side of the bottom row zooms in this $E_{\perp 12}$ interval. As at beam energies around 100A MeV [12], the two event classes are separated

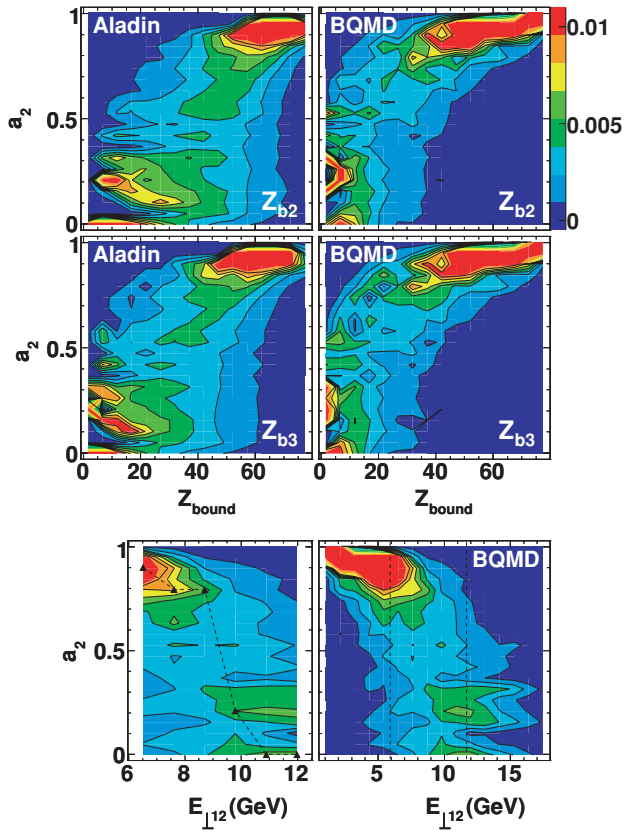

FIG. 8. (Color online) a_2 of the projectile spectator as a function of Z_{b2} (top) and of Z_{b3} (middle) for Au + Au collisions at 600A MeV [33]. On the left-hand side, we show the Aladin experimental results, on the right-hand side the QMD predictions. The bottom row displays the theoretical predictions of a_2 as a function of $E_{\perp 12}$ (right) which are enlarged around intermediate $E_{\perp 12}$ values (delimited by dashed lines) in the left panel. In this latter panel, the symbols show the most probable value of a_2, and the dotted line is to guide the eye.

by a region with $a_2 \approx 0.5$ which contains only a very limited number of events.

V. CONCLUSION

The appearance of two distinct reaction scenarios, multifragmentation and residue production for the *same* value of $E_{\perp 12}$ is a very genuine phenomenon in heavy-ion collisions. It exists over almost the whole energy range for which multifragmentation has been observed, and it exists in participant fragmentation as well as in spectator fragmentation. The fact that physical events show either a small or a large a_2 value but almost never an intermediate a_2 value is first of all remarkable. It is also very general, and the classification of events with the help of a_2 is a good way to elucidate this fact. Whether phase space or nuclear interactions are at the origin of the lack of events with intermediate a_2 values is still unknown.

In the dynamical QMD model, the large impact parameter fluctuations for a given $E_{\perp 12}$ are the reason that events with small and large a_2 values appear for the same value of $E_{\perp 12}$. The data are in agreement with predictions of models which assume that multifragmentation is a fast process. QMD simulations, in which fragments are surviving initial correlations, reproduce the large majority of the experimental observations.

The investigation of the bimodality $E_{\perp 12}$ interval shows that the majority of the events in this interval has properties which are not compatible with the assumptions that large and small a_2 events belong to two phases which exist simultaneously in a small interval of the temperature measured by $E_{\perp 12}$. We cannot, however, exclude that a subset of the events shows the properties expected from a statistically equilibrated system. Investigations whether such a subset can be found have been advanced recently [34]. It would therefore be interesting to see whether such a subset may be a sign of true bimodality, i.e., can be reproduced in statistical models with an energy fluctuation expected for a system having a fixed temperature. Of course generalized statistical ensembles can be defined [35] assuming that in each event E, N, and V differ. It remains to be seen how the distribution of E, N, V can be assessed and whether such an approach is compatible with data.

[1] M. Pichon *et al.* (INDRA and ALADIN Collaboration), Nucl. Phys. **A749**, 93c (2004); **A779**, 267 (2006).
[2] M. Bruno *et al.*, Nucl. Phys. **A807**, 48 (2008).
[3] D. H. E. Gross, cond-mat/0409542v1; D. H. E. Gross and J. F. Kenney, J. Chem. Phys. **122**, 224111 (2005); Ph. Chomaz and F. Gulminelli, Physica A **330**, 451 (2003).
[4] F. Gulminelli and Ph. Chomaz, Nucl. Phys. **A734**, 581 (2004); A. J. McKane and F. Vazquez, Phys. Rev. E **64**, 046116 (2001).
[5] G. Chauduri, S. Das Gupta, and F. Gulminelli, arXiv:0809:0170.
[6] J. P. Bondorf, A. S. Botvina, A. S. Iljinov, I. N. Mishustin, and K. Sneppen, Phys. Rep. **257**, 133 (1995).
[7] D. H. E. Gross, Rep. Prog. Phys. **53**, 605 (1990), and references therein.
[8] J. Aichelin, Phys. Rep. **202**, 233 (1991).
[9] C. Hartnack *et al.*, Eur. Phys. J. A **1**, 151 (1998).
[10] A. Ono and H. Horiuchi, Phys. Rev. C **53**, 2958 (1996).
[11] A. Ono, S. Hudan, A. Chbihi, and J. D. Frankland, Phys. Rev. C **66**, 014603 (2002).
[12] K. Zbiri *et al.*, Phys. Rev. C **75**, 034612 (2007).
[13] A. Le Fèvre and J. Aichelin, Phys. Rev. Lett. **100**, 042701 (2008).
[14] J. Lukasik *et al.*, Phys. Lett. **B566**, 76 (2003); A. Le Fèvre *et al.*, Nucl. Phys. **A735**, 219 (2004).
[15] M. B. Tsang *et al.*, Phys. Rev. Lett. **71**, 1502 (1993).
[16] D. J. Morrissey, Phys. Rev. C **39**, 460 (1989).
[17] M. V. Ricciardi *et al.*, Phys. Rev. Lett. **90**, 212302 (2003).
[18] A. Wieloch *et al.*, Phys. Lett. **B432**, 29 (1998).
[19] M. Hudan, Ph.D. thesis, University of Caen, GANIL T 01 07 (2001).
[20] C. Dorso and J. Randrup, Phys. Lett. **B301**, 328 (1993).
[21] C. Dorso and J. Aichelin, Phys. Lett. **B345**, 197 (1995); J. Aichelin and R. Puri, J. Comput. Phys. **162**, 245 (2000); P. B. Gossiaux, R. Puri, C. Hartnack, and J. Aichelin, Nucl. Phys. **A619**, 379 (1997).

[22] A. S. Goldhaber, Phys. Lett. **B53**, 306 (1974).
[23] A. Andronic, J. Lukasik, W. Reisdorf, and W. Trautmann, Eur. Phys. J. A **30**, 31 (2006).
[24] X. Campi and H. Krivine, Nucl. Phys. **A620**, 46 (1997).
[25] X. Campi, H. Krivine, E. Plagnol, and N. Sator, Phys. Rev. C **67**, 044610 (2003).
[26] D. H. E. Gross *et al.*, Rep. Prog. Phys. **53**, 605 (1990).
[27] R. Nebauer and J. Aichelin, Nucl. Phys. **A681**, 353 (2001).
[28] Ch. Hartnack and J. Aichelin, Phys. Lett. **B506**, 261 (2001).
[29] J. Colin *et al.* (INDRA Collaboration), Phys. Rev. C **67**, 064603 (2003).
[30] P. Kreuz *et al.*, Nucl. Phys. **A556**, 672 (1993).
[31] A. S. Botvina *et al.*, Nucl. Phys. **A584**, 737 (1995).
[32] T. Odeh *et al.*, Phys. Rev. Lett. **84**, 4557 (2000).
[33] A. Schüttauf *et al.*, Nucl. Phys. **A607**, 457 (1996).
[34] E. Bonnet *et al.* (INDRA Collaboration), Phys. Rev. Lett. **103**, 072701 (2009).
[35] M. I. Gorenstein and M. Hauer, Phys. Rev. C **78**, 041902(R) (2008).